A CONTINUOUS FRICTION MODEL FOR SERVO SYSTEMS WITH STICTION

Vahid Johari Majd Marwan A. Simaan
Department of Electrical Engineering
University of Pittsburgh
Pittsburgh, PA 15261

Abstract

In this paper, we introduce a continuous model for friction torque of servo systems which involve stiction at extremely low velocities. This new friction model can be applied to both away from zero and close to zero velocity regimes. For high velocities this model reduces to the classical friction model while for very low velocities it allows for the realization of pre-sliding phenomena without the hysteresis effect.

1.0 Introduction

Friction modeling is an extremely important issue in servo systems with bi-directional tasks. Classical friction models involve hard nonlinearities at zero velocity where friction torque exhibits instantaneous changes in value [1]. However, the discontinuity between the level of static friction torque and Coulomb friction torque in these models has been proven to be unrealistic [2].

In the past decade several friction models which give a smooth transition between the level of static friction torque and Coulomb friction torque have been introduced in the literature [1,3,4]. However, these models still suffer from a discontinuity at zero velocity. Although Dahl [5] earlier proposed a model which yields a continuous torque at zero velocity, his model can't be applied in away from zero velocity regimes, and supports neither viscous friction nor stiction phenomena. Moreover, Dahl's model is computationally intensive due to the fact that it involves a nonlinear differential equation.

In this paper, we introduce a new friction model which can be applied in both close to zero and away from zero velocity regimes. This model features a continuous friction torque at zero velocity which provides a pre-sliding phase similar to that of the Dahl's model.

In section 2, we discuss the classical friction models, the pre-sliding phenomenon, and the Dahl's model. In section 3, we introduce our new friction model which includes a sharpness index at zero velocity, and in section 4 we show that the unknown parameter in our model can be found by numerically solving a nonlinear algebraic equation. In section 5, we show that an approximate analytical solution for the model parameter can also be derived. This considerably enhances the usefulness of this model in formulating the friction for the servo systems with bi-directional tasks.

2.0 Classical Friction Models

It is well known that in a servo system, the total friction torque F can be represented as a nonlinear function of the form

$$F(\omega) = \mathcal{F}(\omega, f_\omega, f_c, f_s) \qquad (1)$$

where ω is the angular velocity, f_ω is the linear viscous friction coefficient, f_c is the steady or Coulomb friction torque, and f_s is the static friction torque. The parameters f_ω, f_c, and f_s are non-negative, and we define the difference $f_s - f_c$ as "stiction" which should be also non-negative (i.e., $f_s \geq f_c$).

Various models for the function $F(\omega)$ have been proposed in the literature [1]. Typically, the shape of $F(\omega)$ depends on the range of velocities within which the servo system operates. For high velocities, the function $F(\omega)$ can be greatly simplified, while in low velocities this function is much more complicated and involves stiction which can not be neglected. The simplest classical model [4] is described by

$$F(\omega) = \begin{cases} f_s \,\mathrm{sign}(\omega) & \text{if } |\omega| < \varepsilon \\ f_\omega \omega + f_c \,\mathrm{sign}(\omega) & \text{otherwise} \end{cases} \qquad (2)$$

where ε is a very small positive value. Figure 1 shows a plot of F versus ω according to this model. From this figure it is clear that the model involves hard nonlinearities at $\omega=0$ where the friction torque instantly jumps from the level of static friction torque f_s to Coulomb friction torque f_c. A control design based on such a model will yield poor system performance in close to zero velocity regimes. Moreover, as reported by Walrath [2], the instantaneous jump from the static friction level to the Coulomb friction level is unrealistic and is not observed in practice. In real applications, there exists a smooth transition between these two levels.

A more accurate model in the form

$$F(\omega) = f_\omega \omega + f_c \,\mathrm{sign}(\omega) + \frac{f_s - f_c}{1 + |\omega/\omega_c|^m} \qquad (3)$$

0-7803-2550-8/95$4.00©1995 IEEE

was later given in the literature [6]. In this model, ω_c is called the critical angular velocity, and m is an empirical positive real number. Another popular model for friction [3] is expressed by

$$F(\omega) = f_\omega \omega + \left[f_c + (f_s - f_c)\, e^{-|\omega/\omega_c|^m}\right]\text{sign}(\omega)$$

where the real number m in the above equation is in the range of $0.5 \le m \le 2$. In most applications, however, the value of m is chosen to be equal to one, and the above expression becomes

$$F(\omega) = f_\omega \omega + \left[f_c + (f_s - f_c)\, e^{-|\omega/\omega_c|}\right]\text{sign}(\omega) \qquad (4)$$

Models (3) and (4) give a smooth transition from the static level of friction to the dynamic level at $\omega=0$ as illustrated in Figure 2. Note that there exists a negative slope for the friction torque for a positive range of velocities close to zero. This is known as Stribeck effect and as pointed out in the literature [1,2,4], is experienced in practical applications, and may produce many side effects [7]. Note that for away from zero velocity regimes (i.e., $|\omega| >> \omega_c$) the three models given in (2), (3), and (4) reduce to

$$F(\omega) = f_\omega \omega + f_c \text{sign}(\omega) \qquad (5)$$

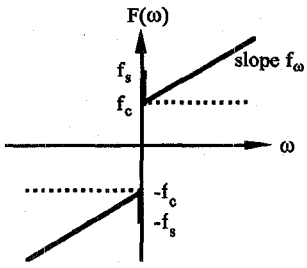

Figure 1. Friction model without Stribeck effect.

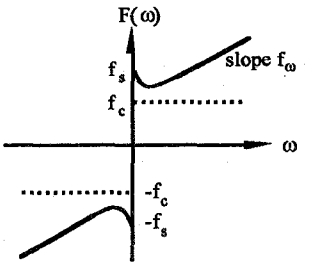

Figure 2. Friction model with Stribeck effect.

In spite of the existence of these models, other researchers [2] have experimentally observed that a relatively small displacement occurs between the contact surfaces of the system even though the applied torque is less than the level of the static friction torque. This phenomenon, called pre-sliding, does not support the discontinuity at zero velocity exhibited in these models. Although the magnitude of the pre-sliding displacement is much smaller than the rolling and sliding displacement, it can easily be transformed into a significant displacement elsewhere in the servo system.

Pre-sliding phenomena can be explained within the framework of the theory of asperity junction adhesion [7]. Asperities between two rubbing surfaces allow for very small displacements, even though the applied torque is less than the level of static friction torque. When the applied torque overcomes the static friction level of the two rubbing surfaces, the asperity junctions break and sliding begins. Dahl proposed a model by which this pre-sliding phenomenon can be realized [5]. The Dahl's model can be described by a nonlinear differential equation which also allows friction hysteresis loop around zero velocity. Figure 3 shows the friction torque at pre-sliding stage versus the angular position, and the hysteresis loop associated with it which takes place as a result of the increase and decrease of the applied torque at velocity reversals.

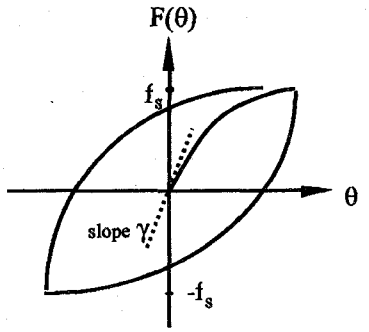

Figure 3. Dahl's friction model.

3.0 A New Friction Model

As mentioned earlier, the classical friction models described in (2)-(4), include Coulomb and static friction torques, but are discontinuous at zero velocity and neglect pre-sliding phenomena. Dahl's model on the other hand, though simulates the pre-sliding displacement, does not include the viscous friction and breakaway torques and is formulated only for slow motion without considering stiction. It also involves a nonlinear differential equation which is difficult to deal with in real time computation. The advantage of Dahl's model is that it gives a continuous friction torque at zero velocity.

In this paper, we propose a new friction model which has the simplicity of classical friction models, but also realizes a continuous friction torque at zero velocities and includes the pre-sliding phenomena as in Dahl's model. Hence, it can be used for both close to zero and away from zero velocity regimes. However, it does not emulate hysteresis which is considered in the Dahl's model.

Our proposed friction model is of the form

$$F(\omega) = f_\omega \omega + \left[f_c + \sigma e^{-|\omega/\omega_c|} - (\sigma + f_c) e^{-|n\omega/\omega_c|}\right]\text{sign}(\omega) \qquad (6)$$

where ω_c is the critical angular velocity, and n is a positive real number which specifies the sharpness of the friction curve at zero velocity. Note that this function is continuous at $\omega=0$ and that, as in all friction models, it has odd symmetry with respect to the $\omega=0$ axis. The parameter σ is a real number to be determined such that

$$\max_{0<\omega<\omega_c} (F^+(\omega)) = f_s \qquad (7)$$

where $F^+(\omega)$ is the friction torque expression for $\omega>0$ which can be written as

$$F^{+}(\omega) = f_{\omega}\omega + f_c + \sigma e^{-\omega/\omega_c} - (\sigma + f_c) e^{-n\omega/\omega_c} \quad (8)$$

It is desired to set f_s equal to the local maximum of this function at a point close to, but slightly larger than, $\omega=0$ as illustrated in the sketch in Figure 4.

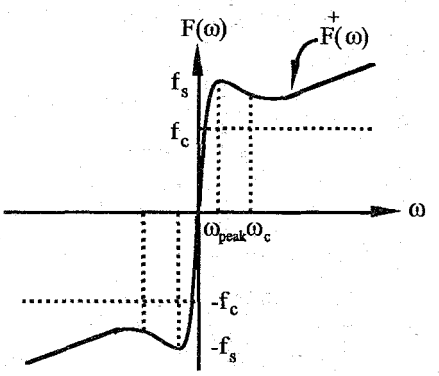

Figure 4. Sketch of $F(\omega)$ of equation (6) versus ω.

4.0 Determination of the Model Parameter

If the condition

$$f_{\omega} << \frac{nf_c}{\omega_c} \quad (9)$$

is satisfied, it can be easily shown (using Taylor series expansion) that for $\omega < \omega_c$ the term $f_{\omega}\omega$ in (8) can be neglected and equation (8) simplifies to

$$F^{+}(\omega) = f_c + \sigma e^{-\omega/\omega_c} - (\sigma + f_c) e^{-n\omega/\omega_c} \quad (10)$$

Maximizing this function by setting $\frac{dF^{+}(\omega)}{d\omega} = 0$ yields

$$-\frac{\sigma}{\omega_c} e^{-\omega/\omega_c} + \frac{n(\sigma + f_c)}{\omega_c} e^{-n\omega/\omega_c} = 0$$

which can be solved for ω_{peak}:

$$\omega_{peak} = \frac{\ln\left[n(1 + \frac{f_c}{\sigma})\right]}{n-1}\omega_c \quad (11)$$

Substituting (11) in (10) yields

$$F^{+}(\omega_{peak}) = f_c + \sigma (n-1) n^{\frac{-n}{n-1}} (1 + \frac{f_c}{\sigma})^{\frac{-1}{n-1}} \quad (12)$$

and making use of (7) we obtain

$$f_s = f_c + \sigma (n-1) n^{\frac{-n}{n-1}} (1 + \frac{f_c}{\sigma})^{\frac{-1}{n-1}} \quad (13)$$

The above nonlinear algebraic equation can be numerically solved for the parameter σ which appears in model (6).

Let us now illustrate the above model with a practical example. Consider the friction model with the following parameters

$$f_{\omega} = .05,\ f_c = .5,\ f_s = 1.9 f_c = .95,\ n = 10,\ \omega_c = .019 \quad (14)$$

Note that these parameters easily satisfy condition (9). Equation (11) and the numerical solution of equation (13) yield

$$\omega_{peak} = 0.006 \quad \text{and} \quad \sigma = 0.6858 \quad (15)$$

Figures 5.a and 5.b show plots of $F(\omega)$ versus ω for the classical model based on equation (4) and the new proposed friction model based on equation (6). As we see from the plots, both models are very close, but unlike the model of equation (4) the proposed friction model is continuous at $\omega=0$. Furthermore, it is clear from Figure 5.a that the linear viscous friction coefficient f_{ω} does not have much influence in the close to zero velocity regime, which is a consequence of condition (9).

As was mentioned earlier, the parameter n can be used to control the sharpness of $F(\omega)$ around $\omega=0$. Figures 6 and 7 illustrate this point. Clearly, a larger value for n results in a sharper slope for friction torque around zero velocity and yields a smaller ω_{peak}. In fact, in the limit, as $n \to \infty$ the new model (6) approaches the classical model (4). Also if we examine this new model in a neighborhood very close to $\omega=0$ as illustrated in Figures 7.a and 7.b, we can observe that the slope of friction torque at $\omega=0$ increases linearly with the increase of the parameter n, while the peak velocity drops in a nonlinear fashion given by (11).

5.0 An Approximate Solution for the Parameter σ

An alternative method for determining the parameter σ is to obtain an approximate analytic solution of equation (13). Let us define δ as the maximum allowable relative error in the friction peak due to the approximation of the parameter σ. In other words, let

$$\left| \frac{F^{+}(\omega_{peak}) - f_s}{f_s} \right| \le \delta \quad (16)$$

As we will show later, for arbitrary small values of δ the above error bound will be satisfied if the sharpness index n is large enough to satisfy the following inequality

$$\left| \frac{(1 + \frac{f_c}{\sigma})^{\frac{-1}{n-1}} - 2^{\frac{-1}{n-1}}}{2^{\frac{-1}{n-1}}} \right| \le \frac{f_s}{f_s - f_c}\delta \quad (17)$$

For the values of n which satisfies (17) we can approximate

$$(1 + \frac{f_c}{\sigma})^{\frac{-1}{n-1}} \approx 2^{\frac{-1}{n-1}} \quad (18)$$

Applying the above approximation into equation (13) yields

$$f_s = f_c + \sigma (n-1) n^{\frac{-n}{n-1}} 2^{\frac{-1}{n-1}}$$

Solving the above equation for the parameter σ, results in

$$\sigma = \frac{(2n^n)^{\frac{1}{n-1}}}{n-1}(f_s - f_c) \quad (19)$$

The above approximate analytic solution for the parameter σ can be directly applied into the proposed friction model (6).

Proposition: If inequality (17) is satisfied, then the parameter σ given in (19) will result in a peak friction $F^+(\omega_{peak})$ which satisfies (16).

Proof: Substituting the approximate solution (19) into (12) gives

$$F^+(\omega_{peak}) = f_c + (f_s - f_c)\frac{\left(1+\frac{f_c}{\sigma}\right)^{\frac{-1}{n-1}}}{2^{\frac{-1}{n-1}}}$$

Rewriting the above equation yields

$$\frac{F^+(\omega_{peak}) - f_s}{f_s} = \frac{f_s - f_c}{f_s}\left[\frac{\left(1+\frac{f_c}{\sigma}\right)^{\frac{-1}{n-1}}}{2^{\frac{-1}{n-1}}} - 1\right] \qquad (20)$$

From inequality (16) we have

$$-\delta \le \frac{F^+(\omega_{peak}) - f_s}{f_s} \le \delta$$

Substituting (20) into the above inequality yields

$$-\delta \le \frac{f_s - f_c}{f_s}\left[\frac{\left(1+\frac{f_c}{\sigma}\right)^{\frac{-1}{n-1}} - 2^{\frac{-1}{n-1}}}{2^{\frac{-1}{n-1}}}\right] \le \delta$$

and considering the fact that $f_s - f_c$ is non-negative, we get

$$-\frac{f_s}{f_s - f_c}\delta \le \frac{\left(1+\frac{f_c}{\sigma}\right)^{\frac{-1}{n-1}} - 2^{\frac{-1}{n-1}}}{2^{\frac{-1}{n-1}}} \le \frac{f_s}{f_s - f_c}\delta$$

or

$$\left|\frac{\left(1+\frac{f_c}{\sigma}\right)^{\frac{-1}{n-1}} - 2^{\frac{-1}{n-1}}}{2^{\frac{-1}{n-1}}}\right| \le \frac{f_s}{f_s - f_c}\delta .$$

Q.E.D.

To find out the least values of parameter n which would satisfy (17), we rewrite the inequality (17) as

$$\left|\left(\frac{1}{2}+\frac{f_c}{2\sigma}\right)^{\frac{-1}{n-1}} - 1\right| \le \frac{f_s}{f_s - f_c}\delta$$

Substituting the approximate solution of parameter σ given by (19) into the above inequality yields

$$\left|\left[\frac{1}{2}+\frac{f_c}{f_s - f_c}\times\frac{n-1}{2(2n^n)^{\frac{1}{n-1}}}\right]^{\frac{-1}{n-1}} - 1\right| \le \frac{f_s}{f_s - f_c}\delta \qquad (21)$$

Now, we define parameter η so that it satisfies

$$f_s = \eta f_c \qquad (22)$$

where we have

$$\eta \ge 1.$$

Thus inequality (21) becomes

$$\left|\left[\frac{1}{2}+\frac{n-1}{2(\eta-1)(2n^n)^{\frac{1}{n-1}}}\right]^{\frac{-1}{n-1}} - 1\right| \le \frac{\eta}{\eta-1}\delta$$

or

$$-\frac{\eta}{\eta-1}\delta \le \left[\frac{1}{2}+\frac{n-1}{2(\eta-1)(2n^n)^{\frac{1}{n-1}}}\right]^{\frac{-1}{n-1}} - 1 \le \frac{\eta}{\eta-1}\delta \qquad (23)$$

The numerical solution of the above condition suggests that the lower bound in inequality (23) is always satisfied when $\eta \ge 1$ (which is always physically true). However the numerical solution for the upper bound in (23) gives an upper bound for η as a function of parameter n.

Figure 8.a illustrates the upper bound for η resulting from the inequality (23) when δ=0.02. This 2% value for δ is a typical choice in many practical engineering design problems. In Figure 8.a the shaded area defines the space (n,η) for which the approximate solution (19) yields a valid friction model. The dashed line in Figure 8.a is the line where both approximate solution and exact solution yield the same value for the parameter σ. This curve can be found by setting δ=0 in the inequality (23). Thus the equation of the dashed curve which yields no approximation error can be written as

$$\left[\frac{1}{2}+\frac{n-1}{2(\eta-1)(2n^n)^{\frac{1}{n-1}}}\right]^{\frac{-1}{n-1}} - 1 = 0$$

or

$$n - 1 - (\eta - 1)(2\,n^n)^{\frac{1}{n-1}} = 0$$

In the example mentioned in the previous part where n=10, the value of parameter η for δ=2% approximation error is 2.3666, and for δ=0% approximation error is 1.6452. Thus for n=10 it is required that $1 \le \eta \le 2.3666$. From f_s and f_c given in (14), we can observe that the value of η in this example falls within the above allowable range.

Figure 8.b shows the approximate as well as the exact solution of parameter σ, normalized by $f_s - f_c$, as a function of parameter n. As we can see from this plot, the approximate solution, shown by the solid line, is very close to the exact solution, depicted by the dashed line. Also it is apparent that the normalized value of parameter σ tends to unity as parameter n tends to infinity. Therefore the parameter σ itself approaches $f_s - f_c$ as n approaches infinity, and consequently the proposed friction model given by the equation (6) approaches the classical model given by the equation (4).

Figure 9.a illustrates the approximate and the exact friction torque of the proposed model for various values of η within the allowable range when n is equal to 10. The peak values for the approximate solution are marked by circles. The first value for η, i.e. η=1.9, is the case

given in the example. The second value, η=1.645, is the case where the approximate solution and the exact solution of σ are identical, and as a result, their corresponding curves are on top of each other. The last value, η=1.01, shows that the model is still valid even for the case that the stiction, that is $f_s - f_c$, is very close to zero. Figure 9.b gives the plots for the approximate model in a wider range of the angular velocity.

Remark: In away from zero velocity regime, or in the case where the stiction phenomenon is not to be considered while a realistic continuous friction model is required, we can simplify our friction model by letting $f_c = f_s$ in (6). This results in η=1. It follows from both equations (13) and (19) that, in this case, we have σ=0. In fact, the approximate solution of σ coincides with the exact solution. Thus the proposed continuous friction model reduces to

$$F(\omega) = f_\omega \omega + f_c\left[1 - e^{-|n\omega/\omega_c|}\right]\text{sign}(\omega)\,. \qquad (24)$$

The above equation can be used in the simulation for away from zero velocity regime as well as in cases where the stiction is not considered for close to zero velocity regimes.

6.0 Summary

In this paper, we introduced a friction model for servo systems with bi-directional tasks which can work for both close to zero and away from zero velocity regimes. In this model the pre-sliding phenomenon is allowed and the friction model is continuous at zero velocity. We introduced an exact and an approximate solution for the parameter of the friction model. While a numerical solution can be generated for the former, an analytical solution was achieved for the latter. we also showed that the new friction model can be further simplified and applied for the case where the stiction is neglected.

References

[1] B. H. Armstrong, *et. al.*, "A Survey of Models, Analysis Tools, and Compensation Methods for the Control of Machines with Friction," *Automatica*, Vol. 30, No. 9, pp. 1083-1138, 1994.

[2] C. D. Walrath, "Adaptive Bearing Friction Compensation Based on Recent Knowledge of Dynamic Friction," *Automatica*, Vol. 20, No. 6, pp. 717-727, 1984.

[3] L. C. Bo and D. Pavelescu, "The Friction-Speed Relation and Its Influence on the Critical Velocity of Stick-Slip Motion," *Wear*, Vol. 82, No. 3, pp. 277-289, 1982.

[4] N. E. Leonard and P. S. Krishnaprasad, "Adaptive Friction Compensation for Bi-Directional Low Velocity Position Tracking," *Proceeding of the 31th IEEE Conference on Decision and Control, Tucson, AZ,* IEEE, Piscataway, NJ, pp. 267-273, 1992.

[5] P. R. Dahl, "Measurement of Solid Friction Parameters of Ball Bearing," *Aerospace Corporation*, pp. 49-60, 1978.

[6] D. P. Hess and A. Soom, "Friction at a Lubricated Line Contact Operating at Oscillating Sliding Velocities," *Journal of Tribology Transactions of the ASME*, Vol. 112, No. 1, pp. 147-152, 1990.

[7] B. H. Armstrong, *Control of Machines with Friction*, Kluwer Academic Publishers, Norwell, MA, 1991.

Figure 5.a Close to zero velocity regime with n=10

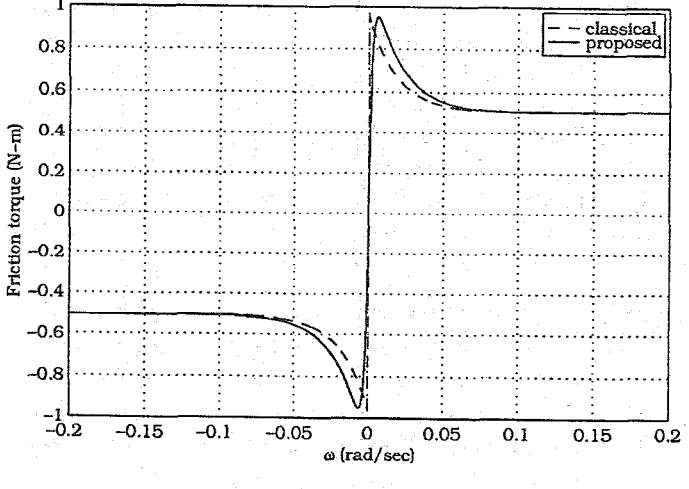

Figure 5.b Away from zero velocity regime

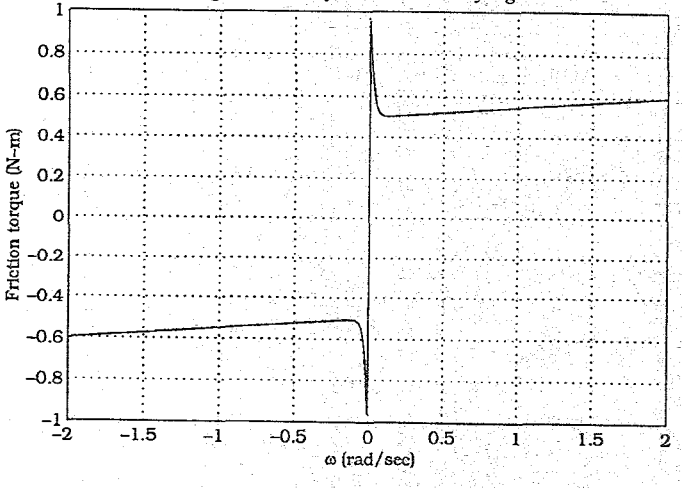

Figure 6. New model for various values of n

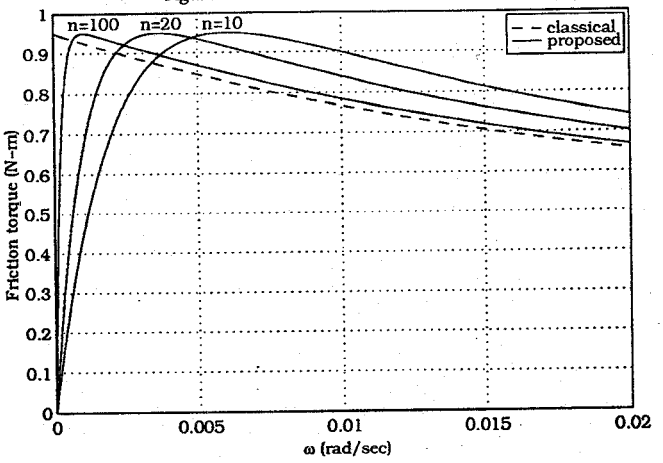

Figure 7.a Friction slope at origin

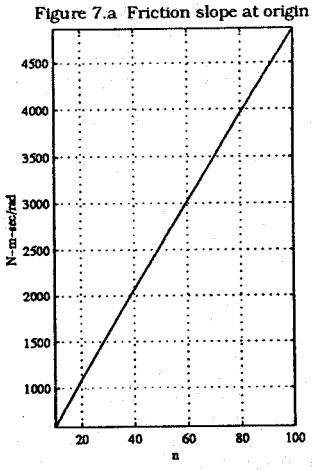

Figure 7.b Peak velocity

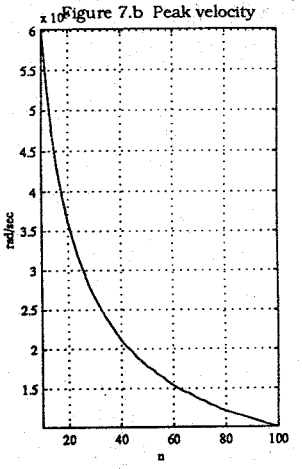

Figure 8.a The allowable values for η (shaded area)

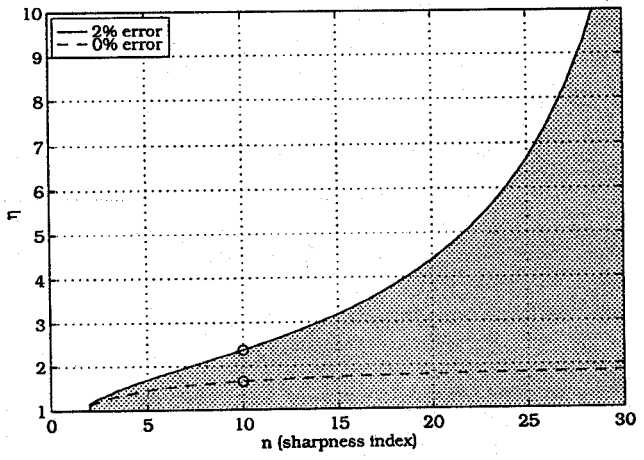

Figure 8.b The normalized value of parameter σ

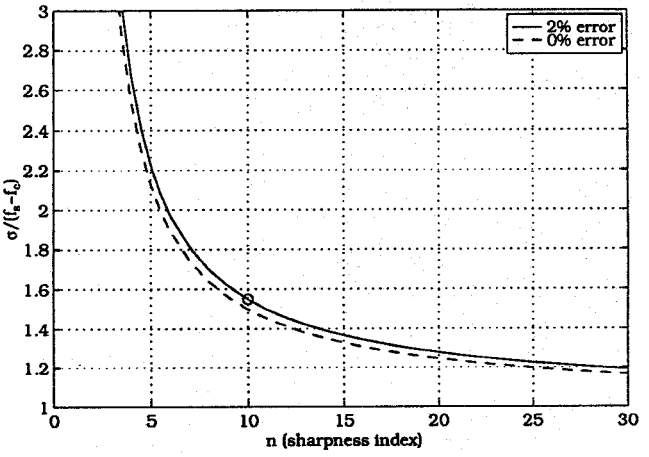

Figure 9.a Variations of the model with n=10 versus parameterη

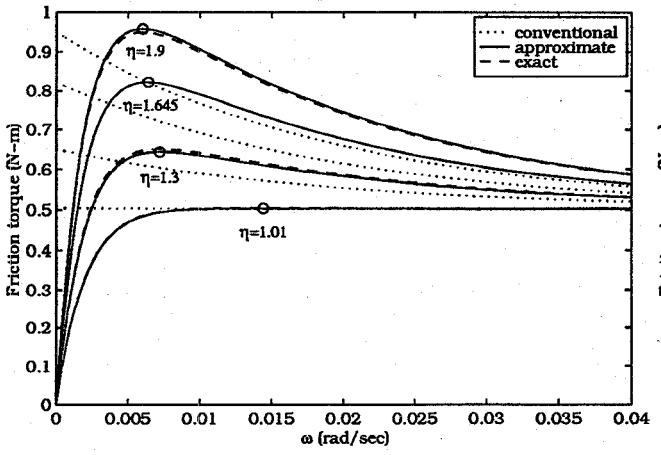

Figure 9.b Variations of approximate model in a wider range